NANO EXPRESS

Crystal Growth of Thiol-Stabilized Gold Nanoparticles by Heat-Induced Coalescence

Sook Young Moon · Shun-ichiro Tanaka ·
Tohru Sekino

Abstract A monolayer of dodecanethiol-stabilized gold nanoparticles changed into two-dimensional and three-dimensional self-organized structures by annealing at 323 K. Subsequent crystal growth of gold nanoparticles occurred. Thiol molecules, although chemisorbed, form relatively unstable bonds with the gold surface; a few thiols desorbed from the surface and oxidized to disulfides at 323 K, because the interaction energy between thiol macromolecules is larger than that between a thiol and a nanoparticle. The gold nanoparticles approached each other and grew into large single or twinned crystals because of the van der Waals attraction and the heat generated by the exothermic formation of disulfides.

Keywords Au · Nanoparticle · Polygon · Coalescence · Dodecanethiol · Surface stabilization · Self-organization

Introduction

Self-organization of nanocrystals has been reported during the past decade. The first two-dimensional (2D) and three-dimensional (3D) superlattices were observed with Ag$_2$S and CdSe nanocrystals, respectively [1–4]. Since then, many researchers have studied various self-organized

S. Y. Moon · S. Tanaka · T. Sekino (✉)
Institute of Multidisciplinary Research for Advanced Materials
(IMRAM), Tohoku University, Katahira 2-1-1, Aoba-ku,
Sendai 980-8577, Japan
e-mail: sekino@tagen.tohoku.ac.jp

S. Y. Moon
The Institute of Scientific and Industrial Research (ISIR), Osaka
University, 8-1 Mihogaoka, Ibaraki, Osaka 567-0047, Japan

lattices of silver [5–14], gold [15–25], cobalt [26, 27], and cobalt oxide [28, 29].

Most superlattice structures have been formed from nanocrystals whose surfaces are covered with alkanethiols. Thiol-stabilized gold nanoparticles [30], including nanocrystals and nanoclusters, have attracted significant research interest in recent years because of their importance in both fundamental science and technological applications such as catalysis, optics, biomedicine, and chemical sensing [31]. Fink et al. [22] investigated characteristic 2D and 3D self-organized structures of surface-modified gold nanoparticles and discussed the importance of their surface chemistry.

Despite the large volume of literature relating to synthesis, morphological development, assembling, and demonstrated applications of thiol-stabilized gold (Au) nanoparticles, only a few studies exist on further structural development such as low-temperature coalescence and grain growth based on self-organized structures. Meli and Green [32] investigated the low-temperature coalescence of self-assembled thiol-stabilized gold nanoparticles in polymer film; however, the thermally induced coalescence to form larger single-crystal particles underwent at 423 K (150°C). Supriya and Claus [33] also reported thermally induced coalescence of thiol-capped gold nanoparticles. However, the phenomenon was observed above 373 K (120°C), which is still rather higher than room temperature.

Recently, we have found, during investigation on the synthesis and self-organization of thiol-stabilized Au nanoparticles, that the prepared Au nanoparticles grew into larger single and/or twinned crystals at relatively low temperature of 323 K (50°C), which is rather near to the room temperature than the previous reports [32, 33]. Here, we describe the growth of thiol-stabilized gold nanoparticles by low-

temperature heat-induced (323 K) coalescence on amorphous carbon film.

Experimental

Thiol-stabilized gold nanoparticles in toluene were prepared by following the literature [34]. Synthesis of thiol-stabilized gold nanoparticles was achieved by reduction of $AuCl_3$ with dodecanethiol as a capping ligand. A 0.025 M micelle solution of *DidodecylDimethylAmmoniumBromide* (DDAB) was prepared in 10 mL toluene. $AuCl_3$ was dissolved in this micelle solution under vigorous stirring, where 0.1 mM of Au^{3+} solution was prepared. Then, freshly prepared sodium borohydride ($NaBH_4$) aqueous solution was added to the former stirred solution drop by drop. The as-formed wine-colored solution was stirred for 2 h at room temperature. The as-prepared gold colloid was split into 5 mL parts, and *1-dodecanethiol* was added to each part, where dodecanethiol/gold mole ratio was varied from 0.8 to 3.2. The gold particles were separated from the solutions by ethanol precipitation to eliminate DDAB, excess thiol and the reaction products. The particles were separated from the supernatant by decanting and vacuum drying. The gold particles were then redispersed in toluene. Gold nanocrystal organizations were prepared via the deposition of dodecanethiol-coated gold nanocrystals onto a copper grid covered with an amorphous carbon film. The grid was immersed in 50 μL of a nanocrystalline solution and kept at 323 K (50°C) and room temperature for a comparison.

The morphology of the particles prepared on the copper grid was directly characterized by transmission electron microscopy (TEM, model H-8100, Hitachi Co., Ltd, Tokyo, Japan) operated at 200 kV. Ultraviolet–visible (UV–vis) spectroscopy (Model 2550, Shimazu, Kyoto, Japan) was used to determine both particle size and degree of aggregation of as-synthesized and annealed particles.

Results and Discussion

Figure 1 shows TEM images of as-prepared gold nanocrystals with various dodecanethiol concentrations. It is clear that synthesized gold nanoparticles self-organized to form a hexagonal close-packed (hcp) structure as schematically indicated in Fig. 1a, b. With increasing dodecanethiol/gold mole ratio from 0.8 to 3.2, the average particle size increased from 5 to 8 nm and the shape changed to dendritic because of the coalescence of neighboring nanocrystals. It has been reported that, generally, larger thiol/gold mole ratios yield smaller average core sizes and more monodisperse particles [35]. In this study,

however, the presence of dodecanethiol in excess, with thiol/gold mole ratio greater than 3.2, yields particle aggregates (Fig. 1c, d). It is thought that the excess thiol ligands have this effect because the sulfur atom of a thiol is quite nucleophilic. Excess thiol ligands in the solution slow the evaporation of toluene, and the interaction between solvent-evaporation kinetics and the excess thiol might cause this aggregation. At a ratio of 0.8, the particle size increased a little (Fig. 1a) because the dodecanethiol molecules may partially cover the gold surface.

Figure 2 shows TEM images of 2D and 3D gold nanocrystals with various annealing times at 323 K. Four samples were prepared simultaneously. After the assigned annealing time, each sample was examined with TEM to observe its general crystal configuration. With increasing annealing time from as-prepared (Fig. 2a) to 24 h (Fig. 2d), the particles aggregated more and more, and finally changed to single or twinned crystals. After annealing for 6 h (Fig. 2b), a small ordered domain formed by the stacking of a few coalesced nanocrystals as shown in Fig. 3, which was somewhat similar to the 3D structure observed by Fink et al. [22]. After annealing for 12 h (Fig. 2c), some nanocrystals coalesced to reach a diameter of ∼20 nm and the initial hexagonal close-packed monolayer organization found in as-synthesized sample (Fig. 2a and also Fig. 1b) was partially disrupted. After annealing for 24 h (Fig. 2d), the coalesced gold nanocrystals continued to grow to form several large (20–60 nm) but triangular single-crystal particles and/or polygons with twinned structures (arrowed in Fig. 2d). Twinned structures are thermodynamically favorable to form decahedral multi-twinned particles [36] and contain more low-energy facets than do single-crystal particles. It has been suggested that atoms on different crystallographic facets might have different interaction strengths with a polymeric or surfactant capping agent, leading to the anisotropic growth of solid materials [37, 38].

UV–vis spectroscopy was used to determine both particle size and degree of aggregation in colloidal particles (Fig. 4). The absorption band, λ_{max} around 500–600 nm, is dependent on the size and shape of the particles, as well as how close they are to each other. Thus, it is useful for identifying not only particle size but also phenomena such as aggregation. The formation of gold nanoparticles through reduction of $AuCl_3$ was examined by observing the change in the absorption band centered at 525 nm originating from the surface plasmon of the gold nanoparticles. With increasing reaction time, the absorption bands redshifted from 525 nm (as-synthesized) to 565 nm (24 h annealing) and the peak sharpness decreased, indicating an increase in particle size.

From this observation, we suggest that the change observed is due to progressive coalescence of the self-
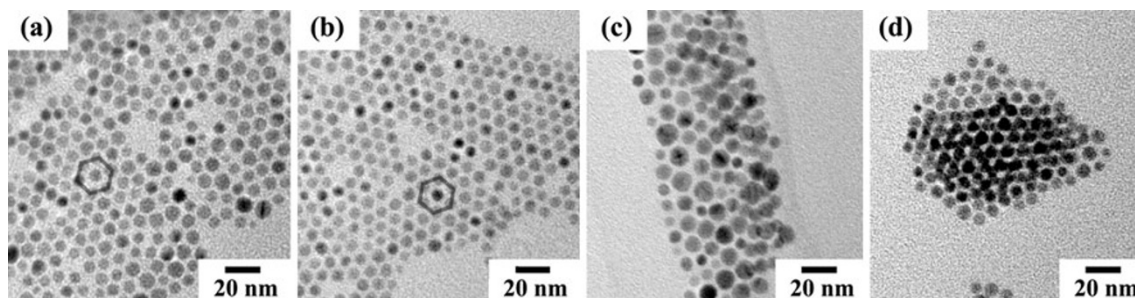
Fig. 1 TEM images of as-prepared 2D-organized gold nanocrystals on amorphous carbon without any heat treatment for various dodecanethiol/ gold ratios: **a** 0.8; **b** 1.6; **c** and **d** 3.2
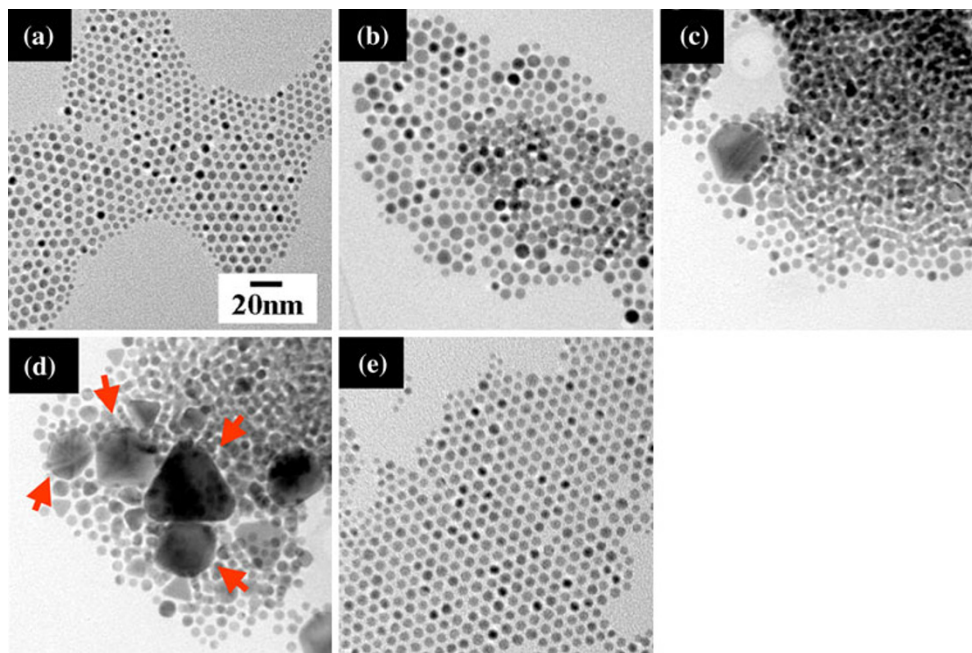
Fig. 2 Effect of annealing time on structural development for 2D and 3D gold nanocrystal organization on amorphous carbon: **a** as-prepared without annealing; annealing at 323 K for **b** 6 h; **c** 12 h; **d** 24 h; **e** soaked at room temperature for 24 h for a comparison. The dodecanethiol/gold ratio is 1.6
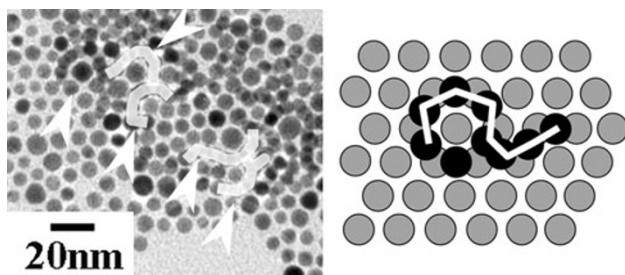
Fig. 3 TEM image and schematic drawing for the formation of 3D structure (monolayer to multilayer) of gold nanoparticles by low-temperature heat treatment at 323 K for 12 h. The dodecanethiol/gold ratio is 1.6

organized 5 nm spherical gold nanoparticles at the rather low temperature of 323 K. However, it should be noted that after soaking at room temperature for 24 h, growth of

organized gold nanoparticles was not observed (Fig. 2e); instead, these nanocrystals grew to another shape during coalescence. The increased interparticle attraction probably arises from thiol desorption. As capping ligands desorb, the steric stability of the nanocrystals decreases and the inclination to aggregate increases. Although the capping ligands chemisorb on the particle surface, the bonds are relatively unstable; at low temperature, the alkyl chains behave as a solid with a rigid configuration, whereas on heating to 323 K, they behave more as a liquid [39]. Pradeep et al. [37] investigated the temperature-dependent phase behavior and dynamic freedom of alkyl chains coated on silver and gold clusters and reported that at 325 K, about 70% of the chains contribute to the dynamic activity. This can also be associated with morphology change similar to our results.
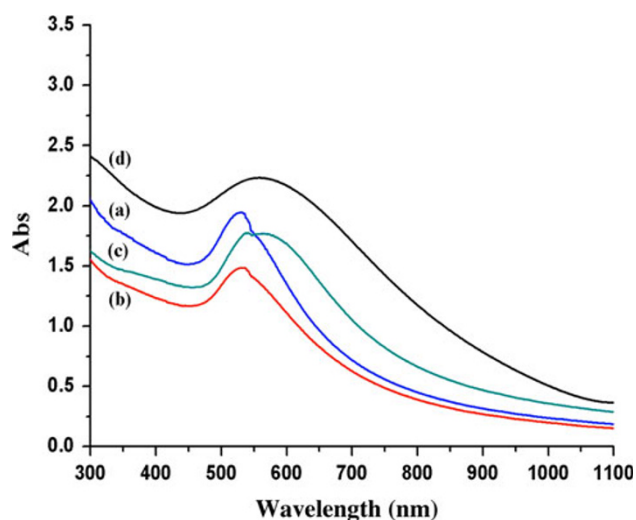
Fig. 4 UV–vis spectra of gold nanocrystals: (*a*) as-prepared and annealed at 323 K for (*b*) 6 h, (*c*) 12 h, and (*d*) 14 h. The dodecanethiol/gold ratio is fixed to 1.6
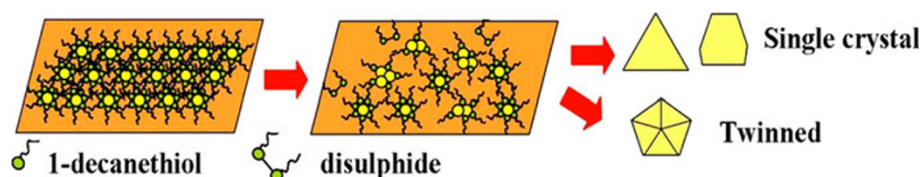
Based on the above-mentioned facts, here, we discuss the plausible mechanism for the 2D organization of thiol-stabilized gold nanoparticles and their coalescence and growth (Fig. 5). The superlattice energy in our case has two components: the thiol–thiol interaction energy ($E_{thiol–thiol}$) and the thiol–nanoparticle interaction energy ($E_{thiol–nanoparticle}$) [40]. The relative values of the two energy components determine the nature of the final structure; specifically, whether it is superlattice, single crystal, and/or twinned crystal. As mentioned earlier, the capping ligands, although chemisorbed, form relatively unstable bonds with the particle surface, and driving forces for both adsorption and desorption exist. A few thiols therefore desorb from the gold surface at 323 K, $E_{thiol–thiol} \gg E_{thiol–nanoparticle}$, and the desorbed thiols oxidize to disulfides [41]. Subsequently, the gold nanoparticles approach each other to form aggregates with partly 3D organization (Fig. 3), and grow into larger single or twinned crystals. The interaction between nanoparticles is strong because of the large polarizability of the gold cores and the consequent van der Waals attraction potential between them. Finally, the gold cores, attracted to each other, grow into other structures such as single and/or twinned crystals (Fig. 2c, d) by the continuously generated

heat from the exothermic formation of disulfides bonds. And hence, the growth must be followed by the diffusion of gold atoms and rearrangement of crystalline lattice. This structure conversion is verified by UV–vis results.

The coalescence mechanism of thiol-stabilized gold nanoparticles in the present study seems to be the same as that recently reported by Meli and Green [32] to some extent; they concluded that, during the initial stage of heating at 423 K, coarsening occurred via simultaneous Ostwald ripening mechanism and coalescence process based upon collision of nanoparticles, whereas during the second stage, coalescence was the dominant mechanism. And they pointed out the importance of desorption of the alkanethiol molecules during the annealing, which associated the transition of two distinct stages. However, it is clearly evident from the present study that thiol-stabilized gold nanoparticles could coalesce to form larger monocrystals at lather low-temperature (323 K, i.e., 50°C), due to the physico-chemical phenomenon as mentioned earlier. The present finding implies us the usefulness and advantage of this method to create self-organized nanoparticulate-derived low-dimensional structures/devices constructed on thermally unstable substrates and/or combined with organic-based functional materials.

Conclusions

In summary, we have devised a method for growing self-organized gold nanoparticles at relatively low temperature (323 K). The morphology of gold nanoparticles was controlled by the presence of dodecanethiol; as the dodecanethiol/gold ratio increased from 0.8 to 3.2, the average particle size increased from 5 to 8 nm at room temperature. The growth of self-organized gold nanoparticles at relatively low temperature (323 K) occurs in three steps: (1) Thiol molecules are desorbed on a gold surface and then oxidized to disulfides. (2) The gold nanoparticle cores approach each other because of van der Waals attraction and then coalesce. (3) The attracting gold cores grow into larger single and/or twinned crystals via the diffusion and rearrangement of gold atoms, because of the heat generated from the exothermic formation of disulfide bonds. We therefore suggest that the dynamic motion of thiol

Fig. 5 Schematic drawing of plausible mechanism for the 2D organization of thiol-stabilized gold nanoparticles and their coalescence and growth to form larger single and/or twinned crystals

molecules is the key to the growth of other shapes and sizes at the processing temperature.

References

1. L. Motte, F. Billoudet, M.P. Pileni, J. Phys. Chem. **99**, 16425 (1995). doi:10.1021/j100044a033
2. C.B. Murray, C.R. Kagan, M.G. Bawendi, Science **270**, 1335 (1995). doi:10.1126/science.270.5240.1335
3. L. Motte, F. Billoudet, E. Lacaze, M.P. Pileni, Adv. Mater. **8**, 1018 (1996). doi:10.1002/adma.19960081218
4. L. Motte, F. Billoudet, E. Lacaze, J. Douin, M.P. Pileni, J. Phys. Chem. B **101**, 138 (1997). doi:10.1021/jp962398k
5. S.A. Harfenist, Z.L. Wang, M.M. Alvarez, I. Vezmar, R.L. Whetten, J. Phys. Chem. **100**, 13904 (1996). doi:10.1021/jp961764x
6. A. Taleb, C. Petit, M.P. Pileni, Chem. Mater. **9**, 950 (1997). doi:10.1021/cm960513y
7. S.A. Harfenist, Z.L. Wang, R.L. Whetten, I. Vezmar, M.M. Alvarez, Adv. Mater. **9**, 817 (1997). doi:10.1002/adma.19970091012
8. P.C. Ohara, J.R. Heath, W.M. Gelbart, Angew. Chem. Int. Ed. Engl. **36**, 1078 (1997). doi:10.1002/anie.199710781
9. S.K. Vijaya, G. Raina, R.T. Yadav, G.U. Kullkarni, C.N.R. Rao, J. Phys. Chem. B **101**, 9876 (1997). doi:10.1021/jp971544z
10. A. Taleb, C. Petit, M.P. Pileni, J. Phys. Chem. B **102**, 2214 (1998). doi:10.1021/jp972807s
11. S.W. Chung, G. Markovich, J.R. Heath, J. Phys. Chem. B **102**, 6685 (1998). doi:10.1021/jp981441w
12. B.A. Korgel, D. Fitzmaurice, Adv. Mater. **10**, 661 (1998). doi:10.1002/(SICI)1521-4095(199806)10:9<661:AID-ADMA661>3.0.CO;2-L
13. Z.L. Wang, S.A. Harfenist, R.L. Whetten, J. Bentley, N.D. Evans, J. Phys. Chem. B **102**, 3068 (1998). doi:10.1021/jp980864v
14. Z.L. Wang, S.A. Harfenist, I. Vezmar, R.L. Whetten, J. Bentley, N.D. Evans, K.B. Alexander, Adv. Mater. **10**, 808 (1998). doi:10.1002/(SICI)1521-4095(199807)10:10<808:AID-ADMA808>3.0.CO;2-R
15. P.C. Ohara, D.V. Leff, J.R. Heath, W.M. Gelbart, Phys. Rev. Lett. **75**, 3466 (1995). doi:10.1103/PhysRevLett.75.3466
16. M. Brust, D. Bethell, D.J. Schiffrin, C. Kiely, Adv. Mater. **7**, 795 (1995). doi:10.1002/adma.19950070907
17. M.J. Hostetler, J.J. Stokes, R.W. Murray, Langmuir **12**, 3604 (1996). doi:10.1021/la960249n
18. R.L. Whetten, J.T. Khoury, M.M. Alvarez, S. Murthy, I. Vezmar, Z.L. Wang, C.C. Cleveland, W.D. Luedtke, U. Landman, Adv. Mater. **8**, 428 (1996). doi:10.1002/adma.19960080513
19. A. Badia, V. Cuccia, L. Demers, F. Morin, R.B. Lennox, J. Am. Chem. Soc. **119**, 2682 (1997). doi:10.1021/ja963571t
20. T.G. Schaff, M.N. Hafigullin, J.T. Khoury, I. Vezmar, R.L. Whetten, W.G. Cullen, P.N. First, W.C. Gutierrez, V. Ascensio, M.J. Ycaman, J. Phys. Chem. B **101**, 7885 (1997). doi:10.1021/jp971438x
21. T. Vossmeyer, S. Chung, W.M. Gelbart, J.R. Heath, Adv. Mater. **10**, 351 (1998). doi:10.1002/(SICI)1521-4095(199803)10:4<351:AID-ADMA351>3.0.CO;2-E
22. J. Fink, C.J. Kiely, D. Bethell, D. Schiffrin, J. Chem. Mater. **10**, 922 (1998). doi:10.1021/cm970702w
23. C.J. Kiely, J. Fink, M. Brust, D. Bethell, D.J. Schiffrin, Nature **396**, 444 (1998). doi:10.1038/24808
24. L.O. Brown, J.E. Hutchison, J. Am. Chem. Soc. **121**, 882 (1999). doi:10.1021/ja983510q
25. X.M. Lin, C.M. Sorensen, K.J. Klabunde, Chem. Mater. **11**, 198 (1999). doi:10.1021/cm980665o
26. C. Petit, A. Taleb, M.P. Pileni, Adv. Mater. **10**, 259 (1998). doi:10.1002/(SICI)1521-4095(199802)10:3<259:AID-ADMA259>3.0.CO;2-R
27. C. Petit, A. Taleb, M.P. Pileni, J. Phys. Chem. B **103**, 1805 (1999). doi:10.1021/jp982755m
28. J.S. Yin, Z.L. Wang, J. Phys. Chem. B **101**, 8979 (1997). doi:10.1021/jp9725285
29. J.S. Yin, Z.L. Wang, Phys. Rev. Lett. **79**, 2570 (1997). doi:10.1103/PhysRevLett.79.2570
30. M. Brust, M. Walker, D. Bethell, D.J. Schiffrin, R. Whyman, J. Chem. Soc. Chem. Commun. **801** (1994). doi:10.1039/c39940000801
31. M. Zhu, C.M. Aikens, F.J. Hollander, G.C. Schatz, R. Jin, J. Am. Chem. Soc. **130**, 5883 (2008). doi:10.1021/ja801173r
32. L. Meli, P.F. Green, ACS Nano **2**, 1305 (2008). doi:10.1021/nn800045s
33. L. Supriya, O.C. Richard, Chem. Mater. **17**, 4325 (2005). doi:10.1021/cm050583h
34. B.L.V. Prasad, S.I. Stoeva, C.M. Sorensen, K.J. Klabunde, Langmuir **18**, 7515 (2002). doi:10.1021/la020181d
35. M.C. Daniel, D. Astruc, Chem. Rev. **104**, 293 (2004). doi:10.1021/cr030698+
36. L.D. Marks, Rep. Prog. Phys. **57**, 603 (1994). doi:10.1088/0034-4885/57/6/002
37. T. Pradeep, S. Mitra, A. Sreekumaran Nair, R. Mukhopadhyay, J. Phys. Chem. B **108**, 7012 (2004). doi:10.1021/jp0369950
38. X.Y. Liu, P. Bennema, Phys. Rev. B **49**, 765 (1994). doi:10.1103/PhysRevB.49.765
39. A. Courty, A.I. Henry, N. Goubet, M.P. Pileni, Nat. Mater. **6**, 900 (2007). doi:10.1038/nmat2004
40. P. Santiago, H.E. Troiani, C. Gutierrez-Wing, J. Ascencio, M.J. Yacaman, Phys. Status Solidi B **230**, 363 (2002). doi:10.1002/1521-3951(200204)230:2<363:AID-PSSB363>3.0.CO;2-Q
41. M. Dasog, R.W.J. Scott, Langmuir **23**, 3381 (2007). doi:10.1021/la0627415